Biogeochemical probing of microbial communities in a basalt-hosted hot spring at Kverkfjöll volcano, Iceland

Running title: Biogeochemistry in a basaltic hot spring

ABSTRACT

We investigated bacterial and archaeal communities along an ice-fed surficial hot spring at Kverkfjöll volcano – a partially ice-covered basaltic volcano at Vatnajökull glacier, Iceland, using biomolecular (16S rRNA, *apsA*, *mcrA*, *amoA*, *nifH* genes) and stable isotope techniques. The hot spring environment is characterized by high temperatures and low dissolved oxygen concentrations at the source (68 °C and <1 mg/l (± 0.1 %)) changing to lower temperatures and higher dissolved oxygen down stream (34.7 °C and 5.9 mg/l), with sulfate the dominant anion (225 mg/l at the source). Sediments are comprised of detrital basalt, low-temperature alteration phases and pyrite, with < 0.4 wt. % total organic carbon (TOC). 16S rRNA gene profiles reveal that organisms affiliated with *Hydrogenobaculum* (54 – 87 % bacterial population) and *Thermoproteales* (35 – 63 % archaeal population) dominate the micro-oxic hot spring source, while sulfur oxidizing archaea (*Sulfolobales,* 57 – 82 %), and putative sulfur oxidizing and heterotrophic bacterial groups dominate oxic downstream environments. The $\delta^{13}C_{org}$ (‰ V-PDB) values for sediment TOC and microbial biomass range from -9.4 ‰ at the spring's source decreasing to -12.6 ‰ downstream. A reverse effect isotope fractionation of ~3 ‰ between sediment sulfide ($\delta^{34}S$ ~0 ‰) and dissolved water sulfate ($\delta^{34}S$ +3.2 ‰), and $\delta^{18}O$ values of ~ -5.3 ‰ suggest pyrite forms abiogenically from volcanic sulfide, followed by abiogenic and microbial

oxidation. These environments represent an unexplored surficial geothermal environment analogous to transient volcanogenic habitats during putative 'snowball Earth' scenarios and volcano-ice geothermal environments on Mars.

1. INTRODUCTION

Hydrothermal systems that exist within glacial settings represent a unique group of microbial habitats at the volcano – cryosphere interface (Cousins *et al*., 2013; Marteinsson *et al*., 2013). These systems typically form in circumpolar volcanically-active regions such as Iceland (Björnsson, 2000) and Antarctica (Soo *et al*., 2009), where ice-capped volcanoes are common. Hot springs also exist in Svalbard, where deep geothermally heated water is released into the perennially cold Arctic environment, producing a unique arctic microbial habitat (Starke *et al*., 2013). Previous studies investigating microbial communities in similar environments have been conducted at geothermal sites in Antarctica, including geothermal soils at Tramway Ridge on Mt. Erebus (Soo *et al*., 2009) and marine hydrothermal sites at Deception Island (Amenábar *et al*., 2013).

Today, such environments are localised and uncommon, but were likely more prevalent during hypothesised "snowball Earth" episodes (Fraser *et al*., 2014), and during periods of volcano – ice interaction on Mars (Cousins & Crawford, 2011). More broadly, terrestrial geothermal environments provide insights into putative early microbial metabolisms and ecological structures on the early Earth (Reysenbach & Cady, 2001), and potential prebiotic chemical pathways. For example, hydrothermal fluids at the Kverkfjöll volcano have been shown to liberate activated phosphorous from schreibersite ($(Fe,Ni)_3P$) – a common mineral in iron-nickel meteorites – as a way to provide biologically-available P to early-Earth environments (Bryant *et al*., 2013, Kee *et*

al., 2013). Basalt-hosted geothermal systems in particular are relevant in this early-Earth context, and also have direct relevance for the upcoming future exploration of Mars, for which ancient areas of putative hot spring activity and hydrothermal alteration are of increasing priority.

The Vatnajökull ice cap in central Iceland overlies several volcanic systems, many of which are associated with geothermal environments ranging from subglacial lakes (Bjornsson, 2000; Gaidos *et al*., 2004, 2008) to surface geothermal fields (Ólafsson *et al*., 2000; Cousins *et al*., 2013). These environments are unstable due to frequent volcanic and seismic activity along this part of the Iceland rift zone, which often results in the rapid drainage of subglacial and ice-dammed lakes (Bjornsson, 2000; Montanaro *et al*., 2016). Previous studies have revealed different physicochemical environments in such subglacial lakes, ranging from cold, oxic, oligotrophic waters at Grimsvötn (Gaidos *et al*., 2004) to anoxic, cold lakes with hydrothermal sulfidic input at Skafta (Jóhannesson *et al*., 2007; Gaidos *et al*., 2008). Microbial communities identified in these lakes were found to be dominated by bacterial groups adapted to oligotrophic and psychrophilic niches and dominated by groups utilising chemolithotrophic metabolisms (Gaidos *et al*., 2004, 2008; Marteinsson *et al*., 2013). These previous studies demonstrate the degree of geothermally-driven environmental variability that can occur within a single ice cap, of which the geothermal environments at Kverkfjöll are a surface manifestation.

The combination of genomic characterisation and stable isotope geochemistry of biomass and associated environmental substrates has proven to be a powerful approach for investigating terrestrial geothermal systems and microbial communities driven by chemolithotrophy (Meyer-Dombard *et al*., 2011). Integrated analysis of carbon, sulfur, and nitrogen isotopic values can indirectly reveal microbial carbon fixation pathways, the prevalence of dissimilatory sulfate reduction or sulfide oxidation, and the importance of microbial nitrogen fixation (e.g. Havig *et al*.,

2011; Loiacono *et al*., 2012; Schubotz *et al*., 2013; Zerkle *et al*., 2016; Havig *et al*., 2017). Likewise, pairing of physicochemical parameters with phylogenetic data has revealed that many hydrothermal microbial assemblages at Yellowstone National Park, USA are bisected by a chemo-photosynthetic 'fringe' defined by a combined effect of temperature, pH, and dissolved sulfide (Boyd *et al.,* 2010; Cox *et al*., 2011; Meyer-Dombard *et al*., 2011). Such studies give a broad, functional view on microbial ecology in terrestrial geothermal systems. Here, we use a combined genomic, stable isotope, and geochemical approach to investigate the microbial communities and their putative biogeochemical cycling within a basalt-hosted geothermal spring habitat in Iceland, which due to its relatively high elevation is disconnected from major sea- or groundwater bodies, allowing geomicrobiology fuelled by local volcanic and glacial inputs to be investigated.

2. FIELD AREA

The Kverkfjöll volcanic system lies along the northern margin of the Vatnajökull ice cap, comprising two subglacial calderas. The western rim of the northernmost caldera (approximately 1600 – 1700 m elevation, Ólafsson *et al*., 2000) is exposed where vigorous geothermal activity interacts with the surrounding ice and surface snow to form a number of hydrothermal areas, dominated by two large (~500 m diameter) ice-dammed lakes – Gengissig (also known as Kverkfjallalón) and Galtarlón. These are surrounded by nearby ephemeral hot springs, mud pots, and fumaroles (Ólafsson *et al*., 2000) ranging in pH from acidic to neutral (Cousins *et al*., 2013). These little-explored hydrothermal systems provide a unique opportunity to investigate the bacterial and archaeal communities that exploit the volcano - ice boundary environment, and more broadly within little-explored basalt-hosted terrestrial geothermal environments. In addition to strong seasonal variations imparted by their high latitude (64 °N), these habitats are also subject

to sudden destructive events, such as the hydrothermal explosion event that was triggered by the sudden and rapid drainage of Gengissig in August 2013 (Montanaro *et al*., 2016). The area investigated (Figure 1) lies within the Gengissig depression that contains an ice-dammed meltwater lake (Montanaro et al., 2016). The hot spring system sampled sits adjacent to the north shore of this lake among an area of geothermally-heated ground, steam-heated pools and fumaroles that are enclosed by ice. We investigated the composition and diversity of bacterial and archaeal communities and their potential biogeochemical cycling of carbon, sulfur, and nitrogen within this single hot spring overflow system prior to the drainage of Gengissig in August 2013 (Montanaro *et al*., 2016).

3. METHODS

3.1 Field sampling

Water, sediment, and biomass samples were collected from a hot spring pool and overflow stream within the Hveradalur geothermal field (64°40.176′ N, 16°41.166′ W) in June 2011. The hot spring system we sampled comprises three interconnected pools of unknown depth, each approximately 10 m in diameter. These pools overflow to form a shallow stream (1 – 4 cm depth) that feeds into Gengissig ice-dammed lake. Samples were taken from the source hot spring pool ("OF0"), and successively downstream along the overflow ("OF1", "OF2", and "OF3") up to 20 m away from the top of the spring pools (Figure 2). In addition, a well-developed microbial mat ("Mat"), microbial streamers and associated mineral crust ("Streamer"), and a red terraced crust plus biomass-rich sediment ("Red Crust") were sampled. Environmental measurements were measured *in situ* at the time of sample collection. These were pH and temperature (VWR PH10 meter,

accuracy ±0.1 for pH and 0.1 °C for temperature), and dissolved oxygen (DO; Mettler Toledo™ FiveGo™ F4 DO Meter, accuracy ± 0.1 %, resolution 0.01 mg/l). Sediment and biomass samples were taken using ethanol-flame sterilized metal spatulas, stored within sterile Whirlpak sample bags on ice for the duration of sampling and transport, followed by storage at -80 °C upon return to the laboratory until analysis. Water samples for geochemical analyses were collected into pre-washed polypropylene bottles and were filtered at the time of collection using a Millex-AP glass fibre prefilter to remove large (>2 μm) particulate matter, then filtered again using Millipore 0.45 μm cellulose acetate filters as described previously (Cousins *et al.,* 2013). Duplicate 30 ml water samples were taken in this manner, one of which was immediately acidified with nitric acid to a final pH <2 for cation analysis. Blank samples of *d*H_2O were also taken. These were all kept cold (~ 4 °C) prior to analysis.

3.2 Dissolved water chemistry

Dissolved ion chemistry of water samples collected from Kverkfjöll in 2011 and associated *d*H_2O field blanks were analyzed with a Dionex Ion Chromatograph and Horoba JY Ultima 2C ICP-AES for dissolved anion and cation analyses respectively, at the Wolfson Geochemistry Laboratory at Birkbeck College/University College London (UCL). Standards were run during analysis for calibration. Cation results were taken as the mean of three repeat measurements, with standard deviation ranging between < 0.01 - 0.3 % (Al, Ca, Fe, K, Mg, P), 0.3 – 0.9 % (Na), and 0.09 – 3.2 % (Si). Dissolved sulfide was assessed qualitatively *in situ* at all sites using a visual methylene blue test (Cline 1969) to identify either a positive or negative detection, with a minimum detection limit of 0.05 mg/l.

3.3 Mineralogical analysis

For bulk mineralogical analysis, sediment samples were freeze-dried and homogenized to <500 μm grain size using an alumina pestle and mortar prior to analysis with a Bruker D8 Advance XRD with a Vantec 1 detector at Aberystwyth University, UK, calibrated using a corundum standard. Sample spectra were compared to mineral spectra using the International Centre for Diffraction Data database, and the RRUFF database (Downs, 2006). Scanning Electron Microscope (SEM) imaging of microtextures and minerals within sediments and microbial mat mineral crusts was achieved using a Jeol Scanning Electron Microscope (JSM-6480LV) at UCL. Samples were gold-coated prior to imaging at an accelerating voltage of 9 keV and working distance of 14 mm.

3.4 DNA extraction from sediments

Total genomic DNA was extracted from sediment and microbial mat samples using the MoBio Powermax DNA Isolation kit (MoBio Laboratories, USA) in accordance with the manufacturer's instructions. Approximately 1 – 5 g (wet weight) of environmental material was used for the extractions, and two separate extractions were pooled for each sample. One of the two extractions replaced the bead-beating step with 30 minutes incubation at 65°C to mitigate extraction bias induced by both harsh and gentle extraction techniques.

3.5 Sequencing of 16S rRNA genes

454 pyrosequencing of 16S rRNA genes was conducted for both Bacteria (primers 28F - GAGTTTGATCNTGGCTCAG and 519R - GTNTTACNGCGGCKGCTG) and Archaea (primers 517F - GCYTAAAGSRNCCGTAGC and 909R - TTTCAGYCTTGCGRCCGTAC) by Research and Testing, (Research and Testing Laboratory of the South Plains, Lubbock, Texas, USA). Between 2000 - 7000 reads per sample were achieved for each 16S rRNA gene assay with an average post-processing read length of 400 bp. Sequence trimming, denoising, and chimera checking were carried out by Research and Testing (Research and Testing Laboratory of the South Plains, Lubbock, Texas, USA) as per their internal protocols (Edgar, 2010, 2011; Edgar *et al*., 2013), and further chimeric sequences were identified using UCHIIME and removed. Following data clean-up and delivery, sequences were trimmed and aligned using MOTHUR filter.seqs and trim.seqs commands, and aligned to the Silva bacteria and archaea databases (Quast *et al*., 2013) using align.seqs. A final sequence screen was done using screen.seqs to remove sequence outliers. Dataset sizes were preserved for individual site samples to avoid significant loss of data through sub-sampling. MOTHUR dist.seqs was used to create a distance matrix for OTU-based analysis. OTU clustering and rarefaction analysis was achieved using MOTHUR cluster.seqs and rarefaction.single commands. Sequences were screened through NCBI BLAST searches to identify the closest taxonomic match for each read.

In addition to 454-pyrosequencing, 16S rRNA gene clone libraries were created for sites OF0, Mat, Red Crust and Streamer. The 16S rRNA gene was amplified from genomic DNA extracted from sediment/biomass using PCR primers 27F and UN1492R within a 50 µl reaction. PCR was carried out as detailed in Table 1. Individual clone libraries consisted of approximately 140 successfully sequenced clones for each sample, and were made and sequenced by Source Bioscience, Nottingham, UK. Sequences were screened for chimeric sequences using UCHIIME,

then trimmed, and aligned using MOTHUR as with 454 sequence analysis. The resulting tree was visualized using the Interactive Tree of Life software (Letunic & Bork, 2016).

3.6 Functional gene assays

To assess the chemolithotrophic metabolic capacity of the communities within the hot spring, extracted DNA for each site was screened for the presence selected metabolic 'marker genes' by PCR (Table 1). Of these, *apsA* (adenosine -5' -phosphosulfate reductase: reduction of sulfate to sulfite, Friedrich 2002), *mcrA* (coenzyme M methyl reductase: final step in methanogenesis in Archaea, and also involved in anaerobic methane oxidation, Knittel & Boetius, 2009), and archaeal *amoA* (alpha-subunit of the ammonia monooxygenase: ammonia oxygenation to nitrate, Pester *et al.,* 2012) produced successful amplicons at either all or some sites. Nitrogen fixation was also investigated by PCR screening for the nitrogenase sub-unit *nifH* gene (Gaby & Buckley, 2012).

3.7 Stable isotope analysis

All sediments and biomats were freeze-dried, powdered, and stored at -20°C prior to analysis. Total Organic Carbon (TOC), Total Sulfur (TS), Total Nitrogen (TN) weight percent analysis and stable isotope values ($\delta^{13}C$, $\delta^{34}S$, $\delta^{15}N$ respectively) were measured from sediment, biofilms, and mineral crusts using Thermo Fisher Scientific™ Delta V Plus IRMS attached to an Elementar™ Vario MICRO™ cube elemental analyzer at the Geophysical Laboratory, Carnegie Institution of Washington, Washington, DC. Dissolved sulfate was precipitated as $BaSO_4$ for measurement of $\delta^{34}S$ and $\delta^{18}O$. $\delta^{34}S$ values were measured as above, while sulfate $\delta^{18}O$ (as $BaSO_4$) analysis was conducted at the Scottish Universities Environment Research Centre, East Kilbride, UK following

the method of Hall *et al*. (1991), and the evolved CO_2 analysed on a VG SIRA 10 mass spectrometer. For TOC $\delta^{13}C$ analysis, sediment samples were treated with acid vapor prior to analysis (no weight difference was observed) and analyzed in pre-baked (550 °C) capsules. All samples were analyzed in triplicate or tin or Ag capsules. Between 1.9 – 20 mg of sample material was analyzed for $\delta^{13}C$ and $\delta^{15}N$ analysis, and 0.12 – 8.7 mg for $\delta^{34}S$ analysis. Stable isotope values are reported in standard delta notation as ‰ variations relative to the Vienna PeeDee Belemnite (PDB) for $\delta^{13}C$ with an analytical uncertainty of ± 0.1 ‰, Vienna Canyon Diablo Troctolite (CDT) for $\delta^{34}S$ with an analytical uncertainty of ± 0.2 ‰, atmospheric N_2 gas (AIR) for $\delta^{15}N$ with an analytical uncertainty of ± 0.2 ‰ and Vienna Standard Mean Ocean Water (SMOW) for $\delta^{18}O$ with an analytical uncertainty of ± 0.3 ‰.

4. RESULTS

4.1 Water and sediment geochemistry and mineralogy

Temperature in the hot spring overflow steadily decreased from 68 °C at the source pool (OF0) to 34.7 °C at the final sampling point 20 m downstream (OF3), with a concurrent increase in dissolved oxygen (DO) from <1 mg/l to 5.9 mg/l (Figure 3). Pool water pH at site OF0 is 4.8, dropping to the lowest pH measured of 3.6 at site OF1 before increasing downstream to pH 4.2 at the most distal site (OF3). Dissolved chemistry along the stream shows the system is dominated by sulfate, which ranges between 218 - 233 mg/l (Table 2). *In situ* concentrations of dissolved sulfide using the methylene blue visual method was below detection. Dissolved cations in all water samples composed of highly-mobile elements leached from the underlying basaltic bedrock (Mg, Ca, Na, Total Si, K), and increased downstream. Total dissolved Si and Cl are both low (90.8 –

119.9 mg/l Total Si and 6.5 – 8.7 mg/l Cl) indicating low water-rock ratios. Sedimentary TOC, TN, and TS all decreased downstream, with the exception of the microbial mat (Mat) and microbial streamer (Streamer) communities that had elevated TC and TN values accordingly.

SEM images of bottom sediments (Figure 4) from the source pool (OF0) and along the overflow stream reveal euhedral cubic pyrite dispersed amongst detrital basalt and associated low-temperature alteration phases including smectite clays, and zeolites. Cubic pyrite is also present within the mineral crust that overlies grey filamentous, microbial streamers at the Streamer site. In contrast to the sedimentary pyrite at all other sites, the pyrite associated with this streamer community is heavily pitted across the mineral surface (Figure 4b). Bulk XRD analysis has been reported in detail by Cousins *et al.* (2013), and show sediments at OF1, OF2, and OF3 comprise anorthite, diopside, smectite clays and pyrite (Figure 4h, i), while OF0 sediments comprise anorthite and pyrite. Streamer mineral crusts consist of pyrite (Figure 4a) while Red Crust mineral terraces (Figure 4d) are composed of iron oxyhydroxide, also seen in SEM analysis (Figure 4e). Sulfate minerals (e.g. gypsum, jarosite etc.) are not detected in any of the sediments or mineral crusts, and along the whole system dissolved SO_4^{2-} decreases with increasing sedimentary FeS_2 (Figure 5).

4.2 Bacterial and Archaeal Communities

The bacterial community composition along the hot spring overflow is split between the micro-oxic source pool (OF0 and Streamer sites) and the increasingly oxic stream overflow (sites OF1, OF2, OF3, Mat, and Red Crust; Figure 6). The bacterial community within the OF0 sediment is dominated by sequences that affiliate with *Aquificae* species, which make up 87 % of

pyrosequence reads, with the remainder comprising *Proteobacteria* (6 %) and *Firmicutes* (5 %) members. The microbial Streamer community also contains *Aquificae* (54 %), in addition to *Chloroflexi* (20 %), *Firmicutes* (19 %) and *Proteobacteria* (5 %). These data are corroborated by the 16S rRNA clone library data (Supplementary File 1), which identify the members of *Aquificae* in OF0 sediment to be *Hydrogenobaculum* species, and the Streamer community to be dominated by *Hydrogenobaculum* (*Aquificae*), *Chloroflexus* (*Chloroflexi*), *Heliobacillus* (Firmicutes) and *Desulfotomaculum* (*Proteobacteria*). By contrast, 454 sequencing shows the hot spring overflow bacterial communities (sites OF1, OF2, and OF3) are dominated by *Proteobacteria* (33 – 68 %), *Bacteriodetes* (2 – 18 %), *Firmicutes* (4 – 14 %), *Deinococcus-Thermus* (0 – 8 %) and *Actinobacteria* (2 – 7 %).

The Mat microbial community, which like the Streamer community lies at the water-air interface, is dominated by sequences that affiliate with *Proteobacteria* (44 % of 454 reads) and *Chloroflexi* (37 % of 454 reads), and includes the only occurrence of cyanobacteria (4 % of 454 reads) at this hot spring system. Sequencing of Mat 16S rRNA clones show the majority of community members are not classifiable with a cultured genera (Supplementary File 1). The phylogenetic relationship revealed by the 16S rRNA clone library sequences show the communities in the Mat sample and Red Crust sediment also have many closely-related members (Figure 7).

The archaeal community (Figure 6c) is dominated by thermophillic groups along the whole system, including *Thermoproteales*, and *Sulfolobales*. *Sulfolobales* in particular dominates community composition (57 – 82 %) in the oxic sites along the stream, with the exception of the Red Crust site, which comprises 73 % *Thaumarchaeota*. *Thermoproteales* are prevalent in the OF0 (35 %) and Streamer (63 %) communities, decreasing gradually downstream. The

Thaumarchaeota in Red Crust sediments most closely match the candidate species *Nitrosocaldus yellowstonii* – an autotrophic aerobic ammonia oxidizing archaeon (de la Torre *et al*., 2008).

4.4 Functional marker genes

Marker genes *apsA* and *nifH* were amplified from all sites along the hot spring overflow with the exception of the microbial Streamer community (negative *apsA*). *dsrAB* was not detected at any of the sites despite multiple attempts. PCR screening for *amoA* produced a positive result at the Red Crust site, consistent with the putative detection of *Nitrosocaldus yellowstonii* in the 16S rRNA gene profiles, while *mcrA* was identified only in OF0 sediments, although it is unclear which 16S phylotypes may be harbouring this gene.

4.5 Stable isotope measurements

$\delta^{13}C$, $\delta^{34}S$, $\delta^{15}N$, and $\delta^{18}O$ stable isotope values are given in Table 3. $\delta^{13}C$ values for TOC within sediments and mineral crusts range between -11.3 to -17.7 ‰, with the microbial streamers at the Streamer site having the least negative $\delta^{13}C$ values (-9.4 ‰). These $\delta^{13}C$ values become increasingly negative from the spring source (OF0) downstream (Figure 8), and correlate with a decrease in sedimentary TOC. $\delta^{34}S$ values for bulk TS within sediment (pyrite), biomass, and mineral crusts (pyrite) have isotopic compositions very close to 0 ‰ along the whole system (-0.8 to -0.2 ‰), with the exception of the Red Crust and Streamer material, for which $\delta^{34}S$ values are markedly more positive (+2.4 to +5.2 ‰). A $\Delta^{34}S_{SULFATE\text{-}PYRITE}$ value of +3.5 ‰ was measured between the sedimentary pyrite and the dissolved fluid sulfate $\delta^{34}S$ values, which themselves range between +2.9 to +3.4 ‰ along the system (Figure 8). $\delta^{18}O$ values for the sulfate-bound oxygen

($\delta^{18}O_{SULFATE}$) are consistently -5.2 to -5.4 ‰ along sites OF0, OF1, OF2 and OF3 (Figure 8). Finally, sedimentary TN $\delta^{15}N$ values fall between -1.55 and +0.42 ‰, while biomass TN $\delta^{15}N$ values range down to -2.39 ‰ (Streamer) and -0.8 ‰ (see Table 3). All sediment/crust TOC has $C/N_{(at)}$ ranging between 6.5 and 11.8, while biomass from the Mat and Streamer material ranges between 6.3 and 9.4 (all standard deviations of replicate analyses < ±0.9).

5. DISCUSSION

5.1 Carbon and Nitrogen cycling

The autotrophic *Hydrogenobaculum* and facultative autotrophic *Chloroflexus* communities at the hydrothermal pool (OF0) are likely to be fixing volcanic CO_2 delivered to the pool via fumaroles (80 – 97 % fumarole gas, Ólafsson *et al*., 2000). $\delta^{13}C$ values for fumarolic CO_2 at Kverkfjöll have been previously measured as -4.1 ‰, consistent with a MORB magmatic origin (Poreda *et al*., 1992; Ármannsson, 2016). The fractionation between volcanogenic CO_2 and TOC ($\Delta^{13}C_{TOC\text{-}CO2}$) therefore ranges from -5.3 to -13.6 ‰. The small $\Delta^{13}C_{TOC\text{-}CO2}$ values of -5.3 to -7.2 ‰ at the Streamer and OF0 sites respectively are consistent with fractionations observed for the reductive tricarboxylic acid (rTCA; *Hydrogenobaculum*) and 3-hydroxypropionate (3-HP; *Chloroflexus*) carbon fixation pathways (~2 – 13 ‰ for rTCA and <7 ‰ for 3-HP, House *et al*., 2003; Zerkle *et al.,* 2005). The *mcrA* gene was successfully amplified at the OF0 site, indicating that methanogenesis, anaerobic oxidation of methane (AOM), or alkane oxidation (Laso-Perez *et al.,* 2016) could be employed here. A $\delta^{13}C_{TOC}$ value of -11.3 ‰ rules out substantial methanogenesis or AOM activity, for which a considerably more negative $\delta^{13}C_{TOC}$ value would be recorded in the resulting biomass, especially for AOM (Zerkle *et al*., 2005). Finally, the change in microbial

phylotypes from chemolithoautotrophic bacterial groups at the source hydrothermal pool (OF0) to chemoheterotrophic groups downstream (Sites OF1, OF2, and OF3, Figure 6) corresponds with the increasingly negative $\delta^{13}C_{TOC}$ values (Figure 8). These potentially record a shift in metabolic strategy as environmental conditions (e.g., DO and temperature) change downstream, but further investigation would be required to elucidate active carbon fixation pathways. Despite permissive temperatures and pH (Boyd et al., 2010; Cox *et al.,* 2011) across the whole system, the occurrence of phototrophic phylotypes in the *16S rRNA* gene profiles were restricted to the microbial communities at the Streamer (*Chloroflexi*) and Mat (*Chloroflexi* and *Cyanobacteria* groups) sites. This suggests phototrophy does not play a major role in primary productivity in these environments. The sites explored however occupy a pH – temperature window for which the occurrence of phototrophy in hot springs has not been well-defined, due to the relative rarity of hot springs with this range (pH 3-5; < 50 °C; Cox *et al.,* 2011), and the 'patchy' distrubition of phototrophy identified at pH <5 and <56 °C (Boyd *et al.,* 2012).

TN $\delta^{15}N$ values of -2.39 ‰ to -0.8 ‰ are consistent with $\delta^{15}N$ values produced through nitrogen fixation via nitrogenase (Zhang *et al.,* 2014), and the detection of *nifH* at all sites shows microbial nitrogen fixation is functionally possible within these communities. The identification of the archaeal *amoA* marker gene in Red Crust sediment is in agreement with the dominance of *Thaumarchaeota* members within the 16S rRNA gene profile, which most closely match the candidate species *Nitrosocaldus yellowstonii* – a thermophilic ammonia oxidizing archaeon (de la Torre *et al*., 2008). However beyond these observations, it is not possible to elucidate any active N cycling pathways. As such, the fixation, speciation, and localised biogeochemical cycling of N in these habitats warrants further study, given these local heterogeneities, and the exogenous inputs of N as part of the wider glacial biogeochemistry (*e.g.* Hodson et al., 2005).

5.2 Sulfur and Iron cycling

The relatively enriched $\delta^{34}S_{PYRITE}$ values indicate that microbial sulfate reduction was not involved in the generation and subsequent precipitation of sulfide, because microbial sulfate reduction is associated with significant (-20 to -4 ‰) isotope fractionation. Instead, $\delta^{34}S_{PYRITE}$ values are consistent with MORB values of − 0.9 ± 0.5 ‰ (Labidi *et al*., 2012) and Icelandic basaltic bedrock sulfide values of -2 to +0.4 ‰ (Torssander, 1989). The precipitation of pyrite, then, follows an abiogenic pathway, whereby volcanogenic H_2S (1 - 12 % fumarole gas, Ólafsson *et al*., 2000) immediately reacts completely with dissolved iron in the spring water upon mixing, consistent with the lack of detection of dissolved sulfide within the near-surface water. Complete abiotic oxidation of this pyrite would similarly produce $\delta^{34}S_{SULFATE}$ values consistent with $\delta^{34}S_{PYRITE}$, as there is little fractionation of sulfur isotopes during abiotic oxidative weathering when oxygen is not limited (Taylor *et al*., 1984; Balci *et al*., 2007) and only small (~ -0.7 ‰) fractionation effects observed for pyrite oxidation in micro-oxic aqueous environments, both abiotically and in the presence of *Acidithiobacillus ferrooxidans* (Balci *et al*., 2007). Alternatively values may be expected to record a normal isotope effect of -5.2 ‰ (Fry *et al*., 1988). Instead, a small enrichment in ^{34}S is observed, producing $\delta^{34}S_{SULFATE}$ values of +2.9 to +3.4 ‰, comparable to sulfur oxidation fractionation values (Fry et al., 1984; Smith et al., 2015). While this relatively enriched sulfate could potentially be a residual sulfate pool produced through microbial sulfate reduction, the lack of corresponding negative $\delta^{34}S_{PYRITE}$ values, and negative detection of the *dsrAB* gene by PCR suggests this is not the case. Abiotic oxidation of pyrite is typically a slow process in aqueous environments (Nordstrom & Southam, 1997), allowing sulfide oxidising bacteria and archaea to make use of this substrate. As such, the $\delta^{34}S_{SULFATE}$ values could be feasibly produced via

microbial sulfide oxidation (either using O_2 or NO_3^-). The observed drop in water pH from 4.8 at site OF0 to 3.6 downstream (Figure 3g) at OF1 is consistent with activity of sulfur- and sulfide-oxidising archaeal phylotypes identified at the Mat and OF1-3 sites (Figure 6). Microbial sulfide oxidation activity is also supported by the presence of extensive surface pits on pyrite grains that are in close spatial association with the Streamer microbial community (Figure 4b,c). Such features are known to be produced by microbial oxidation of pyrite (Edwards *et al*., 1999). Finally, the inverse isotope effect from sulfide to sulfate is consistent with known biological sulfide oxidation, for which previous fractionation of up to +3.5 ‰ has been observed in green sulfur bacteria and purple sulfur bacteria (Fry *et al*., 1986; Zerkle *et al*., 2009). However neither of these bacterial groups were identified in the 16S rRNA sequence data, although that is not to say that the sulfide oxidising bacteria and archaea that are present could not also produce this effect. The loss of ^{34}S-depleted SO_2 gas from the incomplete abiogenic oxidation of pyrite to sulfate would also produce an enrichment of ^{34}S in the resulting sulfate (Brunner *et al*., 2008). As such, the observed positive $\delta^{34}S_{SULFATE}$ values could be due to either abiogenic and biological sulfide oxidation. However, biological sulfide oxidation would be consistent with the occurrence of sulfur-utilising bacterial and archaeal phylotypes (e.g. *Hydrogenobaculum, Thiomonas, Thiobacillus, Caldisericum, Sulfolobales),* which suggests microbial sulfur cycling plays an active and important role in the biogeochemistry of these environments.

The Red Crust mineral precipitates are accompanied by an increase in dissolved SO_4^{2-} and a decrease in total dissolved Fe (Figure 3b and f) in the spring water at this site, with the latter removed via oxidation into insoluble Fe-oxyhydroxides, forming the red mineral crust terraces observed (Figure 4d, e, and f). This observation could be caused either by the water becoming locally more oxygenated through atmospheric mixing, or via Fe^{3+} precipitation mediated by iron

oxidizing bacteria or the presence of biomass (Konhauser, 1998; Inskeep *et al*., 2004) due to the acidic pH of the overflow waters (pH 3.6 – 4.2). The ratio between ferrous and ferric Fe can be variable at this pH range (Kaasalainen *et al.,* 2017), and along the rest of the stream total dissolved Fe otherwise increases steadily, showing the precipitation of Fe-oxyhydroxides at Red Crust to be a localised occurrence. *Gallionella* species (7 clones) were identified in the 16S rRNA gene clone library for Red Terrace, and potentially could be playing an active role in the oxidation of iron. Likewise, a large number of *Thiomonas* clones (47 clones) identified suggests oxidation of inorganic sulfur compounds may play an additional role at this site.

Finally, while $\delta^{18}O_{SULFATE}$ values cannot be use to definitively identify an abiotic or biogenic process (Balci *et al*., 2007), the disparity between the $\delta^{18}O_{SULFATE}$ values and the isotopic composition for water at Kverkfjöll ($\delta^{18}O_{H2O}$ = -13.8±3 ‰: Ólafsson *et al*., 2000) suggests pyrite oxidation occurred with the majority of the oxygen atoms taken from water-bound oxygen, and a minor component from dissolved atmospheric O_2. This observation is in agreement with experimental $\delta^{18}O_{SULFATE}$ and $\delta^{18}O_{H2O}$ experiments from biological and abiotic oxidation of pyrite by O_2 by Balci *et al*. (2007), albeit at lower pH, which also indicates that between 85 – 92 % of sulfate-bound oxygen in the Kverkfjöll dissolved SO_4^{2-} is likely to have come from H_2O. These observations are consistent with other geothermally-influenced glacial meltwater $\delta^{18}O_{SULFATE}$ measurements taken elsewhere in Iceland (Wynn *et al*., 2015).

5.3 Relevance to glacial ecosystems on Earth and beyond

The hot spring stream environment investigated in this study represents an isolated hydrothermal habitat within a wider glacial setting. It is likely that such environments are highly localised;

previous δD and $\delta^{18}O$ analysis of fumarole and water samples at Kverkfjöll (Ólafsson *et al*., 2000) show a steady shift away from the meteoric line towards heavier $\delta^{18}O$ values, indicating localised circulation and boiling of fluids and associated water-rock interaction with limited meteoric re-charge (Ármannsson, 2016). This is consistent with the permeable nature of the largely hyaloclastite edifice that makes up the Kverkfjöll massif (Ólafsson *et al*., 2000), aiding shallow fluid circulation. It is therefore possible that the microbial communities inhabiting the surface (and shallow crustal) geothermal environments at Kverkfjöll are largely disconnected from other subglacial hydrothermal ecosystems elsewhere within Vatnajökull, such as those within the subglacial lakes at Grimsvotn and Skafta (Gaidos *et al*., 2004, 2008; Marteinsson *et al*., 2013), which do appear to be hydrologically-connected (Marteinsson *et al*., 2013). Secondly, the subglacial lakes were found to be dominated by a largely cold-adapted bacterial community (Gaidos *et al*., 2008), whereas the Kverkfjöll hot spring system at Hveradalur is dominated by many thermophilic phylotypes in both the bacterial and archaeal communities (Supplementary File 1). Overall, this demonstrates that hydrothermally-driven microbial consortia within Vatnajökull are subject to both top-down (Kverkfjöll) and bottom-up (Skafta, Grimsvotn; Marteinsson *et al*., 2013) colonisation.

Potentially once-habitable aqueous conditions have been identified on Mars that were capable of supporting chemolithoautotrophy (Grotzinger *et al*., 2014). The chemolithoautotrophic microbial communities driven by volcanic CO_2 and sulfide at Kverkfjöll can therefore act as a 'biological analogue' to such past habitats on either early Earth or Mars. As such, efforts in astrobiology should be directed towards biosignatures produced via H- and S-driven chemolithotrophy, and their manifestation within the mineral phases deposited within the associated sedimentary deposits. While the past martian nitrogen cycle is still largely undefined, ~2% N_2 is present in the martian

atmosphere today (Mahaffy *et al*., 2013) and nitrate has been identified in martian soils (Stern *et al*., 2015). Likewise, $C/N_{(at)}$ values for sediment TOC at all of our sample sites are consistent with microbially derived organic matter (Cleveland & Liptzin, 2007), and therefore offer a natural analogue for understanding how microbial life on Mars might record stable isotope biosignatures within preserved organic matter.

CONCLUSIONS

Through this study we combined stable isotope geochemistry with biomolecular analysis to provide an overview of the putatively volcanically-driven biogeochemical processes within a basalt-hosted hydrothermal environment in Iceland. Our study at Kverkfjöll reveals volcano – ice interaction hot spring environments where microbial communities are associated with localised primary volcanic input to the surface environment, particularly utilisation of volcanic CO_2. We characterised bacterial and archaeal community profiles that included site-specific S- and H-driven chemolithoautotrophic and chemoheterotrophic phylotypes. Phylotypes utilising anoxygenic photosynthesis were only present in localised microbial biofilms. The largely ice-bound nature of the hydrothermal environments at Kverkfjoll, coupled with geographic isolation, makes this site an ideal natural laboratory for investigating biogeochemical volatile cycling within a basaltic volcanic setting.

ACKNOWLEDGEMENTS

This work was funded by a The Leverhulme Trust Research Project Grant to I. Crawford (F/07 112/AA). C. Cousins is funded by a Royal Society of Edinburgh Research Fellowship. Stable

isotope analyses at the Carnegie Institution of Washington, USA were funded by a grant from the W. M. Keck Foundation (2007-6-29) and through the NASA Astrobiology grant (NNH082ZDA0002C) to M. Fogel. The authors would like to thank Þorsteinn Þorsteinsson, Magnús Thor Karlsson, Terrence Kee, Barry Herschey, Laura Carmody, and the Icelandic Glaciological Society for field assistance at Kverkfjöll in June 2011. We are grateful to the Icelandic Research Council and the Nature Conservation Agency for permission to undertake research in northern Iceland. Finally, we thank Aubrey Zerkle for helpful comments on the manuscript prior to submission, and the anonymous reviewers for their constructive feedback.

REFERENCES

Abed RM, Garcia-Pichel F, Hernández-Mariné M (2002) Polyphasic characterization of benthic, moderately halophilic, moderately thermophilic cyanobacteria with very thin trichomes and the proposal of Halomicronema excentricum gen. nov., sp. nov. *Archives of Microbiology* **177**, 361-370.

Amenábar MJ, Flores PA, Pugin B, Boehmwald FA, Blamey JM (2013) Archaeal diversity from hydrothermal systems of Deception Island, Antarctica. *Polar Biology* **36**, 373-380.

Anesio AM, Laybourn-Parry J (2012) Glaciers and ice sheets as a biome. *Trends in Ecology & Evolution* **27**, 219-225.

Ármannsson H (2016) The fluid geochemistry of Icelandic high temperature geothermal areas. *Applied Geochemistry* **66**, 14-64.

Arsène-Ploetze F, Koechler S, Marchal M, Coppée J-Y, Chandler M, Bonnefoy V *et al*. (2010) Structure, function, and evolution of the *Thiomonas* spp. genome. *PLoS Genet.* **6**, e1000859.

Balci N, Shanks WC, Mayer B, Mandernack KW (2007) Oxygen and sulfur isotope systematics of sulfate produced by bacterial and abiotic oxidation of pyrite. *Geochimica et Cosmochimica Acta* **71,** 3796-3811.

Barns SM, Fundyga RE, Jeffries MW, Pace NR (1994) Remarkable archaeal diversity detected in a Yellowstone National Park hot spring environment. *Proc Natl Acad Sci USA* **91**, 1609–1613.

Björnsson H (2002) Subglacial lakes and Jökulhlaups in Iceland. *Global and Planetary Change* **35**, 255–271.

Bowman J. (2006) The methanotrophs—the families *Methylococcaceae* and *Methylocystaceae*. In: Dworkin M, Falkow S, Rosenberg E, Schleifer KH, Stackebrandt E (eds), *The Prokaryotes: A Handbook on the Biology of Bacteria*, 3rd edn, vol. 5. Springer: New York, pp 266–289.

Boyd ES, Hamilton TL, Spear JR, Lavin M, Peters JW (2010) [FeFe]-hydrogenase in Yellowstone National Park: evidence for dispersal limitation and phylogenetic niche conservatism. *The ISME Journal* **4**, 1485–1495.

Boyd ES, Fecteau K, Havig JR, Shock EL, Peters JW. (2012) Modeling the habitat range of phototrophic microorganisms in Yellowstone National Park: Toward the development of a comprehensive fitness landscape. *Frontiers in Microbiological Chemistry* **3**, doi: 10.3389/fmicb.2012.00221.

Brunner B, Yu JY, Mielke RE, MacAskill JA, Madzunkov S, McGenity TJ, Coleman M. (2008) Different isotope and chemical patterns of pyrite oxidation related to lag and exponential growth phases of Acidithiobacillus ferrooxidans reveal a microbial growth strategy. *Earth and Planetary Science Letters* **270**, 63-72.

Bryant DE, Greenfield D, Walshaw R.D., Johnson BRG, Herschy B, Smith C, Pasek MA, Telford R, Scowen I, Munshi T, Edwards HGM, Cousins CR, Crawford IA, Kee TP (2013) Hydrothermal modification of the Sikhote-Alin iron meteorite under low pH geothermal environments. A plausable prebiotic route to activated phosphorus on the early Earth. *Geochimica et Cosmochimica Acta* **109**, 90 – 112.

Cleveland CC, Liptzin D (2007) C:N:P stoichiometry in soil: is there a ‘‘Redfield ratio’’ for the microbial biomass? *Biogeochemistry* **85**, 235–252.

Cline J. (1969) Spectrophotometric determination of hydrogen sulfide in natural waters. *Limnology and Oceanography*, **14**, 454-458.

Cockell CS, Pybus D, Olsson-Francis K, Kelly L, Petley D, Rosser N, Howard K, Mosselmans F (2011) Molecular characterization and geological microenvironment of a microbial community inhabiting weathered receding shale cliffs. *Microbial ecology* **61**, 166-181.

Cousins CR, Crawford IA (2011) Volcano–ice interaction as a microbial habitat on Earth and Mars. *Astrobiology* **11**, 695–710

Cousins CR, Crawford IA, Carrivick JL, Gunn M, Harris J, Kee TP, Karlsson M, Carmody L, Cockell C, Herschy B, Joy KH (2013) Glaciovolcanic hydrothermal environments in Iceland and implications for their detection on Mars. *Journal of Volcanology and Geothermal Research* **256**, 61-77.

Cox A, Shock EL, Havig JR (2011) The transition to microbial photosynthesis in hot spring ecosystems. *Chemical geology* **280**, 344-351.

De la Torre JR, Walker CB, Ingalls AE, Könneke M, Stahl DA. Cultivation of a thermophilic ammonia oxidizing archaeon synthesizing crenarchaeol (2008) *Environmental Microbiology* **10**, 810-818.

DeLong EF (1992) Archaea in coastal marine environments. *Proc. Natl. Acad. Sci. U.S.A*. **89**, 5685–5689.

Downs RT (2006) The RRUFF Project: an integrated study of the chemistry, crystallography, Raman and infrared spectroscopy of minerals. Program and Abstracts of the 19th General Meeting of the International Mineralogical Association in Kobe, Japan (O03-13).

Edwards KJ, Goebel BM, Rodgers TM, Schrenk MO, Gihring TM, Cardona MM, Mcguire MM, Hamers RJ, Pace NR, Banfield JF (1999) Geomicrobiology of pyrite (FeS2) dissolution: case study at Iron Mountain, California. *Geomicrobiology Journal* **16**, 155-179.

Einarsson P, Sæmundsson K (1987) Earthquake epicenters 1982–1985 and volcanic systems in Iceland (map). In: Sigfússon I (ed) Í hlutarins eðli, Festschrift for Þorbjörn Sigurgeirsson. Menningarsjóður, Reykjavík.

Fraser CI, Terauds A, Smellie J, Convey P, Chown SL (2014) Geothermal activity helps life survive glacial cycles. *Proc. Natl. Acad. Sci. U.S.A*. **111**, 5634-5639.

Friedrich MW (2002) Phylogenetic Analysis Reveals Multiple Lateral Transfers of Adenosine-5′-Phosphosulfate Reductase Genes among Sulfate-Reducing Microorganisms. *Journal of Bacteriology* **184**, 278-89.

Fry B, Gest H, Hayes JM (1984) Isotope effects associated with the anaerobic oxidation of sulfide by the purple photosynthetic bacterium, Chromatium vinosum. *FEMS Microbiology Letters* **22**, 283–287.

Fry B, Cox J, Gest H, Hayes JM (1986) Discrimination between 34S and 32S during bacterial metabolism of inorganic sulfur compounds. *Journal of Bacteriology* **165**, 328-30.

Fry B, Ruf W, Gest H, Hayes JM (1988) Sulfur isotope effects associated with oxidation of sulfide by O2 in aqueous solution. *Chemical Geology* **73**, 205-210.

Gaby JC, Buckley DH (2012) A Comprehensive Evaluation of PCR Primers to Amplify the nifH Gene of Nitrogenase. *PLoS ONE* **7,** e42149.

Gaidos E, Lanoil B, Thorsteinsson T, Graham A, Skidmore M, Han S-K, Rust T, Popp B (2004) A Viable Microbial Community in a Subglacial Volcanic Crater Lake, Iceland. *Astrobiology* **4**, 327–344.

Gaidos E, Marteinsson V, Thorsteinsson T, Johannesson T, Runarsson AR, Stefansson A, Glazer B, Lanoil B, Skidmore M, Han S, Miller M, Rusch A, Foo W (2008) An oligarchic microbial assemblage in the anoxic bottom waters of a volcanic subglacial lake. *Nature ISME Journal* **3**, 486–497.

Grotzinger JP, Sumner DY, Kah LC, Stack K, Gupta S, Edgar L, Rubin D, Lewis K, Schieber J, Mangold N, Milliken R (2014) A habitable fluvio-lacustrine environment at Yellowknife Bay, Gale Crater, Mars. *Science* **343**, p. 1242777.

Hall AJ, Boyce AJ, Fallick AE, Hamilton PJ (1991) Isotopic evidence of the depositional environment of Late Proterozoic stratiform barite mineralisation, Aberfeldy, Scotland. *Chemical Geology* **87**, 99-114.

Hall JR, Mitchell, KR, Jackson-Weaver O, Kooser AS, Cron BR, Crossey LJ, Takacs-Vesbach CD (2008) Molecular characterization of the diversity and distribution of a thermal spring microbial community by using rRNA and metabolic genes. *Applied and environmental microbiology* **74**, 4910-4922.

Hallbeck L, Pedersen K (1991) Autotrophic and mixotrophic growth of Gallionella ferruginea. *Microbiology* **137**, 2657-2661.

Havig JR, Raymond J, Meyer-Dombard DR, Zolotova N, Shock EL (2011) Merging isotopes and community genomics in a siliceous sinter-depositing hot spring, *J. Geophys. Res.,* **116**, G01005.

Havig JR, Grettenberger C, Hamilton TL (2017) Geochemistry and microbial community composition across a range of acid mine drainage impact and implications for the Neoarchean-Paleoproterozoic transition, *JGR Biogeosciences* **122**, 1404–1422.

Hodson AJ, Mumford PN, Kohler J, Wynn PM (2005) The High Arctic glacial ecosystem: new insights from nutrient budgets, *Biogeochemistry* **72,** 233–256.

House CH, Schopf JW, Stetter KO (2003) Carbon isotopic fractionation by Archaeans and other thermophilic prokaryotes. *Organic Geochemistry* **34**, 345-356.

Jóhannesson T, Thorsteinsson T, Stefánsson A, Gaidos EJ, Einarsson B (2007) Circulation and thermodynamics in a subglacial geothermal lake under the Western Skaftá cauldron of the Vatnajökull ice cap, Iceland. *Geophysical Research Letters* **34** (19).

Kaasalainen H, Stefánsson A, Druschel GK (2017) Geochemistry and speciation of Fe(II) and Fe(III) in natural geothermal water, Iceland.

Kee TP, Bryant DE, Herschy B, Marriott KER, Cosgrove NE, Pasek MA, Atlas ZD, Cousins CR (2013) Phosphate Activation via Reduced Oxidation State Phosphorus (P). Mild Routes to Condensed-P Energy Currency Molecules. Special Issue "Prebiotic Chemistry: Chemical Evolution of Organics on the Primitive Earth", *Life* **3**, 386-402.

Kersters K, Lisdiyanti P, Komagata K, Swings J (2006) The family *Acetobacteraceae*: the genera *Acetobacter*, *Acidomonas*, *Asaia*, *Gluconacetobacter*, *Gluconobacter* and *Kozakia*. In: Dworkin M, Falkow S, Rosenberg E, Schleifer K-M, Stackebrandt E, editors. *The prokaryotes* 3rd ed. New York: Springer. pp. 163–200.

Kim YJ, Nguyen NL, Weon HY, Yang DC (2013) Sediminibacterium ginsengisoli sp. nov., isolated from soil of a ginseng field, and emended descriptions of the genus Sediminibacterium

and of Sediminibacterium salmoneum. *International journal of systematic and evolutionary microbiology* **63**, 905-912.

Knittel K, Boetius A (2009) Anaerobic Oxidation of Methane: Progress with an Unknown Process. *Annu. Rev. Microbiol.* **63**, 311–334.

Konhauser KO (1998) Diversity of bacterial iron mineralization. *Earth Science Reviews* **43**, 91-121.

Kuever J (2014) The family Syntrophobacteraceae. In: Rosenberg E et al (eds) *The Prokaryotes* - Deltaproteobacteria and Epsilonproteobacteria. Springer, Berlin, pp 45.

Labidi J, Cartigny P, Birck JL, Assayag N, Bourrand JJ (2012) Determination of multiple sulfur isotopes in glasses: A reappraisal of the MORB δ 34 S. *Chemical Geology* **334**, 189-98.

Laso-Pérez R, Wegener G, Knittel K, Widdel F, Harding KJ, Krukenberg V et al. (2016). Thermophilic archaea activate butane via alkyl-coenzyme M formation. *Nature* **539**, 396–401.

Letunic I, Bork P (2007) Interactive Tree Of Life (iTOL): an online tool for phylogenetic tree display and annotation. *Bioinformatics* **23**, 127-8.

Loiacono ST, Meyer-Dombard DAR, Havig JR, Poret-Peterson AT, Hartnett HE, Shock EL (2012) Evidence for high-temperature in situ nifH transcription in an alkaline hot spring of Lower Geyser Basin, Yellowstone National Park. *Environmental microbiology* **14,** 1272-1283.

Mahaffy PR, Webster CR, Atreya SK, Franz H, Wong M, Conrad PG, Harpold D, Jones JJ, Leshin LA, Manning H, Owen T (2013) Abundance and isotopic composition of gases in the martian atmosphere from the Curiosity rover. *Science* **341**, 263-266.

Marteinsson VT, Runarsson A, Stefánsson A, Thorsteinsson T, Johannesson T, Magnusson SH, Reynisson E, Einarsson B, Wade N, Morrison HG, Gaidos E (2013) Microbial communities in the subglacial waters of the Vatnajökull ice cap, Iceland. *Nature ISME Journal* **7,** 427-437.

Meyer-Dombard DR, Shock EL, Amend JP (2005) Archaeal and bacterial communities in geochemically diverse hot springs of Yellowstone National Park, USA. *Geobiology* **3**, 211-227.

Meyer-Dombard DR, Swingley W, Raymond J, Havig J, Shock EL, Summons RE (2011) Hydrothermal ecotones and streamer biofilm communities in the Lower Geyser Basin, Yellowstone National Park. *Environmental Microbiology* **13**, 2216–2231.

Miroshnichenko ML, Rainey FA, Hippe H, Chernyh NA, Kostrikina NA and Bonch-Osmolovskaya EA (1998) Desulfurella kamchatkensis sp. nov. and Desulfurella propionica sp. nov., new sulfur-respiring thermophilic bacteria from Kamchatka thermal environments. *International Journal of Systematic and Evolutionary Microbiology* **48**, 475-479.

Moreira D, Amils R (1997) Phylogeny of Thiobacillus cuprinus and other mixotrophic thiobacilli: proposal for Thiomonas gen. nov. *International Journal of Systematic and Evolutionary Microbiology* **47**, 522-528.

Mori K, Yamaguchi K, Sakiyama Y, Urabe T, Suzuki KI (2009) Caldisericum exile gen. nov., sp. nov., an anaerobic, thermophilic, filamentous bacterium of a novel bacterial phylum, Caldiserica phyl. nov., originally called the candidate phylum OP5, and description of Caldisericaceae fam. nov., Caldisericales ord. nov. and Caldisericia classis nov. *International journal of systematic and evolutionary microbiology* **59**, 2894-2898.

Montanaro CB, Scheu B, Gudmundsson MT, Vogfjord K, Reynolds HI, Durig T, Strehlow K, Rott S, Reuschle T, Dingwell DB (2016) Multidisciplinary constraints of hydrothermal explosions based on the 2013 Gengissig lake events, Kverkfjöll volcano, Iceland. *Earth and Planetary Science Letters* **434**, 308-319.

Nakatsu CH, Hristova K, Hanada S, Meng XY, Hanson JR, Scow KM, Kamagata Y (2006) Methylibium petroleiphilum gen. nov., sp. nov., a novel methyl tert-butyl ether-degrading methylotroph of the Betaproteobacteria. *International journal of systematic and evolutionary microbiology* **56**, 983-989.

Nobre MF, Triiper H, da Costa MS (1996) Transfer of Thermus ruber (Loginova et al. 1984), Thermus silvanus (Tenreiro et al. 1995), and Thermus chliarophilus (Tenreiro et al. 1995) to

Meiothermus gen. nov. as Meiothermus ruber comb. nov., Meiothermus silvanus comb. nov., and Meiothermus chliarophilus comb. nov., respectively, and emendation of the genus Thermus. *Int. J. Syst. Bacterial*. **46**, 604-606.

Nordstrom DK, Southam G (1997) Geomicrobiology of sulfide mineral oxidation. *Reviews in mineralogy* **35**, 361-90.

Ólafsson M, Torfason H, Grönvold K (2000) Surface exploration and monitoring of geothermal activity in the Kverkfjöll geothermal area, central Iceland. *Proceedings World Geothermal Congress 2000*, Kyushu-Tohohu, Japan, pp. 1539–1545.

Pester M, Rattei T, Flechl S, Grongroft A, Richter A, Overmann J, Reinhold-Hurk B, Loy A, Wagner M (2012) amoA-based consensus phylogeny of ammonia-oxidizing archaea and deep sequencing of amoA genes from soils of four different geographic regions. *Environ Microbiol* **14**, 525–539.

Poreda RJ, Craig H, Arnorsson S, Welhan JA (1992) Helium isotopes in Icelandic geothermal systems: I. 3 He, gas chemistry, and 13 C relations. *Geochimica et cosmochimica acta* **56**, 4221-4228.

Pujalte MJ, Lucena T, Ruvira MA, et al. The family Rhodobacteraceae. In: Rosenberg G, DeLong EF, Lory S, et al., editors. Prokaryotes: Alphaproteobacteria and Betaproteobacteria. Heidelberg, Berlin: Springer; 2014. p. 439-512.

Quast C, Pruesse E, Yilmaz P, Gerken J, Schweer T, Yarza P, Peplies J, Glöckner FO (2013) The SILVA ribosomal RNA gene database project: improved data processing and web-based tools. *Nucl. Acids Res.* **41**, D590-D596.

Reysenbach AL, Cady SL (2001) Microbiology of ancient and modern hydrothermal systems. *Trends in microbiology* ***9***, 79-86.

Romano C, D'Imperio S, Woyke T, Mavromatis K, Lasken R, Shock EL, McDermott TR (2013) Comparative genomic analysis of phylogenetically closely related Hydrogenobaculum sp. isolates from Yellowstone National Park. *Applied and environmental microbiology* **79**, 2932-2943.

Scholten JCM, Joye SB, Hollibaugh JT, Murrell JC (2005) Molecular Analysis of the Sulfate Reducing and Archaeal Community in a Meromictic Soda Lake (Mono Lake, California) by Targeting 16S rRNA, mcrA, apsA, and dsrAB Genes. *Microbial ecology* **50**, 29-39.

Schubotz F, Meyer-Dombard DR, Bradley AS, Fredricks HF, Hinrichs K-U, Shock EL, Summons, RE (2013) Spatial and temporal variability of biomarkers and microbial diversity reveal metabolic and community flexibility in Streamer Biofilm Communities in the Lower Geyser Basin, Yellowstone National Park. *Geobiology* **11**, 549-569.

Shock EL, Holland M, Meyer-Dombard D, Amend JP (2005) Geochemical sources of energy for microbial metabolism in hydrothermal ecosystems: Obsidian Pool, Yellowstone National Park,

USA. Geothermal Biology and Geochemistry in Yellowstone National Park (eds: Inskeep WP, McDermott TR). Thermal Biology Institute, Montana State University, pp. 95–112.

Smith DA, Steele A, Bowden R, Fogel ML (2015) Ecologically and geologically relevant isotope signatures of C, N, and S: okenone producing purple sulfur bacteria part I. *Geobiology* **13**, 278-291.

Solorzano L (1969) Determination of NH4+ in natural water by the phenolhypochlorite method. *Limnology and Oceanography* **14**, 799–801.

Soo RM, Wood SA, Grzymski JJ, McDonald IR, Cary SC (2009) Microbial biodiversity of thermophilic communities in hot mineral soils of Tramway Ridge, Mount Erebus, Antarctica. *Environmental microbiology* **11**, 715-728.

Starke V, Kirshtein J, Fogel ML, Steele A (2013) Microbial community composition and endolith colonization at an Arctic thermal spring are driven by calcite precipitation. *Environmental microbiology reports* **5**, 648-59.

Stern JC, Sutter B, Freissinet C, Navarro-González R, McKay CP, Archer PD, Buch A, Brunner AE, Coll P, Eigenbrode JL, Fairen AG, Franz HB, Glavin DP, Kashyap S, McAdam AC, Ming DW, Steele A, Szopa C, Wray JJ, Martín-Torres FJ, Zorzano M-P, Conrad PG, Mahaffy PR, Team TMS, Stern J (2015) Evidence for indigenous nitrogen in sedimentary and aeolian deposits from the curiosity rover investigations at Gale crater, Mars. *Proc Natl Acad Sci* **112**, 4245–4250.

Taylor BE, Wheeler MC, Nordstrom DK (1984) Stable isotope geochemistry of acid mine drainage: Experimental oxidation of pyrite. *Geochimica et Cosmochimica Acta* **48**, 2669-2678.

Torssander P (1989) Sulfur isotope ratios of Icelandic rocks. *Contrib. Mineral. Petrol*. **102**, 18-23.

Van Der Meer MTJ, Schouten S, De Leeuw JW, Ward DM (2000) Autotrophy of green non-sulphur bacteria in hot spring microbial mats: biological explanations for isotopically heavy organic carbon in the geological record. *Environmental Microbiology* **2**, 428–435.

Wadham JL, Bottrell S, Tranter M, Raiswell R (2004) Stable isotope evidence for microbial sulphate reduction at the bed of a polythermal high Arctic glacier. *Earth and Planetary Science Letters* ***219***, 341-355.

Wagner ID, Zhao W, Zhang CL, Romanek CS, Rohde M, Wiegel J (2008) Thermoanaerobacter uzonensis sp. nov., an anaerobic thermophilic bacterium isolated from a hot spring within the Uzon Caldera, Kamchatka, Far East Russia. *International journal of systematic and evolutionary microbiology* **58**, 2565-2573.

Watson SW, Bock E, Valois FW, Waterbury JB, Schlosser U (1986) Nitrospira marina gen. nov. sp. nov.: a chemolithotrophic nitrite-oxidizing bacterium. *Archives of Microbiology* **144**, 1-7.

Weisburg WG, Barns SM, Pelletier DA, Lane DJ (1991) 16S ribosomal DNA amplification for phylogenetic study. *J. Bacteriol*. **173**, 697–703.

Willems A, De Ley J, Gillis M, Kersters K (1991) Comamonadaceae, a new family encompassing the acidovorans rRNA complex, including variovorax paradoxus gen. nov., comb. nov., for Alcaligenes paradoxus (Davis 1969). *International Journal of Systematic and Evolutionary Microbiology* **41**, 445-450.

Wynn PM, Morrell DH, Tuffen H, Barker P, Tweed FS, Burns R (2015) Seasonal release of anoxic geothermal meltwater from the Katla volcanic system at Sólheimajökull, Iceland. *Chemical Geology* **396**, 228-238.

Zerkle AL, House CH, Brantley SL (2005) Biogeochemical signatures through time as inferred from whole microbial genomes. *American Journal of Science* **305**, 467-502.

Zerkle AL, Farquhar J, Johnston DT, Cox RP, Canfield DE (2009) Fractionation of multiple sulfur isotopes during phototrophic oxidation of sulfide and elemental sulfur by a green sulfur bacterium. *Geochimica et Cosmochimica Acta* **73**, 291-306.

Zerkle AL, Jones DS, Farquhar J, Macalady JL (2016) Sulfur isotope values in the sulfidic Frasassi cave system, central Italy: A case study of a chemolithotrophic S-based ecosystem. *Geochimica et Cosmochimica Acta* **173**, 373-386.

Zhang X, Sigman DM, Morel FMM, Kraepiel AML (2014) Nitrogen isotope fractionation by alternative nitrogenases and past ocean anoxia. *Proc. Natl. Acad. Sci. U.S.A*. **111**, 13.

FIGURES

Figure 1. (a) Simplified map showing the location of the Kverkfjöll volcanic area (red box, detailed in (b)) in Iceland (active volcanic rift zone shown in green, glaciers in white; adapted and simplified from Einarsson and Sæmundsson, 1987); and **(b)** location of ice-dammed lake Gengessig (red arrow) on the northwest margin of the northern Kverkfjöll caldera (dashed line). The geothermal field (star) sits adjacent to the shore of the lake. Contour lines given in meters.

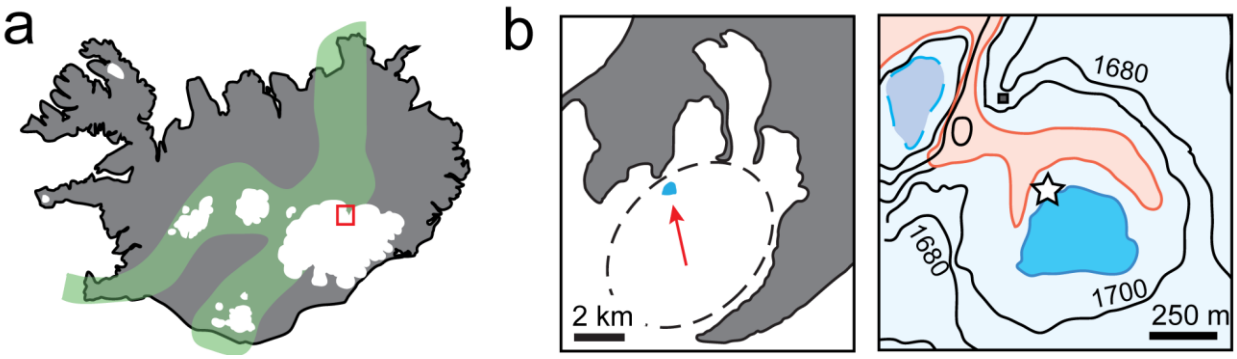

Figure 2. (a) Field photograph of the ice-bound geothermal area adjacent to Gengissig ice-dammed lake (~500 m diameter). **(b)** Field photograph of the hot spring pool and sampling locations Streamer, OF0, Red Crust, and OF1, looking north; distance between sites OF0 and Red Crust is 5 m. **(c)** Field photograph further downsteam along the pool overflow showing sampling locations OF1, Mat, OF2 and OF3, looking south; distance between sites OF2 and OF3 is 3 m. **(d)** Map of the hot spring at Hveradalur showing location of sampling sites along the overflow stream. Direction of flow is top to bottom.

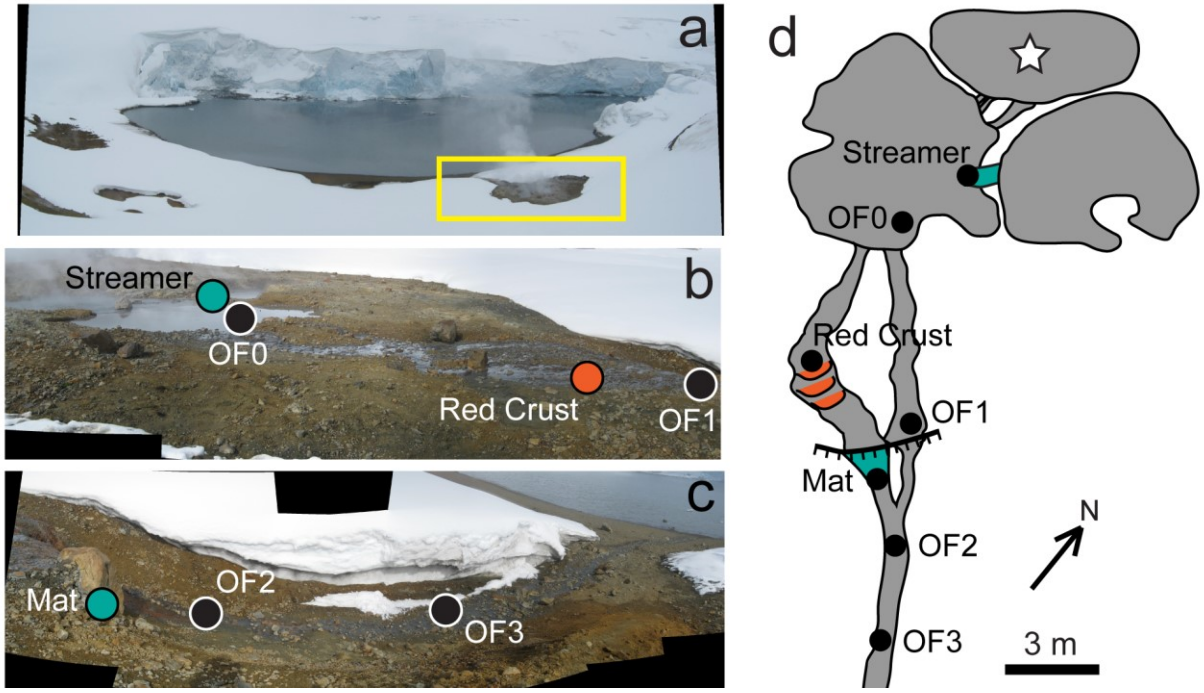

Figure 3. Physicochemical measurements as a function of distance from the top of the pool (star, Figure 2), for sites OF0-OF3 (black), Steamer crust (grey) and biomass (green); Red Crust (orange), and Mat (green). **(a)** sedimentary wt. % TOC; **(b)** total dissolved sulfate; **(c)** temperature; **(d)** dissolved oxygen; **(e)** sedimentary wt. % TS; **(f)** dissolved Total Fe (circles) and Total P (squares); **(g)** water pH; **(h)** dissolved Total Si (circles) and Na (squares). Localised decrease in dissolved Total Fe and P, and corresponding increase in dissolved sulfate at the Red Crust site 11 m downstream is highlighted in grey. Error bars represent standard deviations of replicate analyses, with the majority smaller than the point symbol.

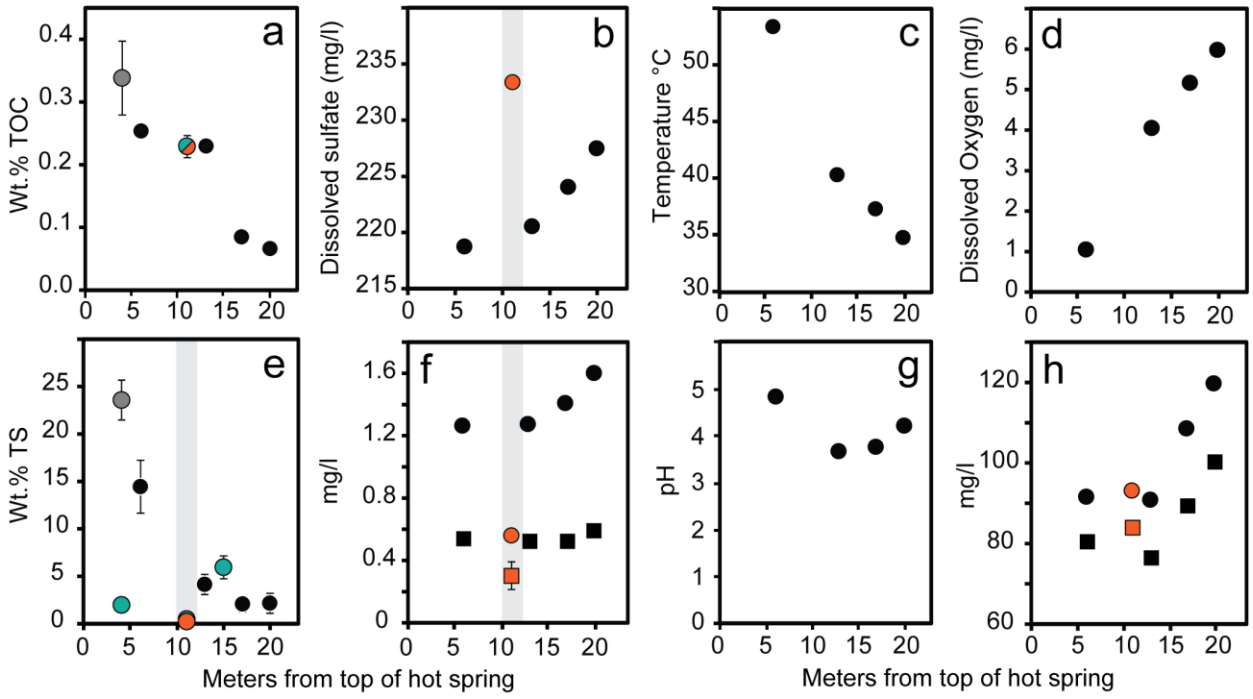

Figure 4. Field images, SEM, XRD, and visible-near infrared (VNIR) reflectance spectra of selected sites along the hydrothermal system. **(a)** 'Streamer' – orange mineral encrusted filamentous grey streamers; **(b and c)** SEM images of pitted cubic pyrite crystals and filamentous structures embedded within the 'Streamer' orange crust; **(d, e, andf)** 'Red Crust' – red mineral crusts overlying red wet sediment and biomass; SEM image of microcrystalline iron oxides that make up the red terraces ; and VNIR reflectance spectra of crust and underlying sediment/biomass; **(g)** 'OF2' overflow site '17 m from the top of the pool system (star, Figure 2); **(h)** SEM image of cubic pyrite within 'OF3' overflow site 20m from the top of the pool system; **(i)** SEM image of basaltic grains with alteration minerals in sediment from the'OF2' overflow site, 17 m from the top of the pool system.

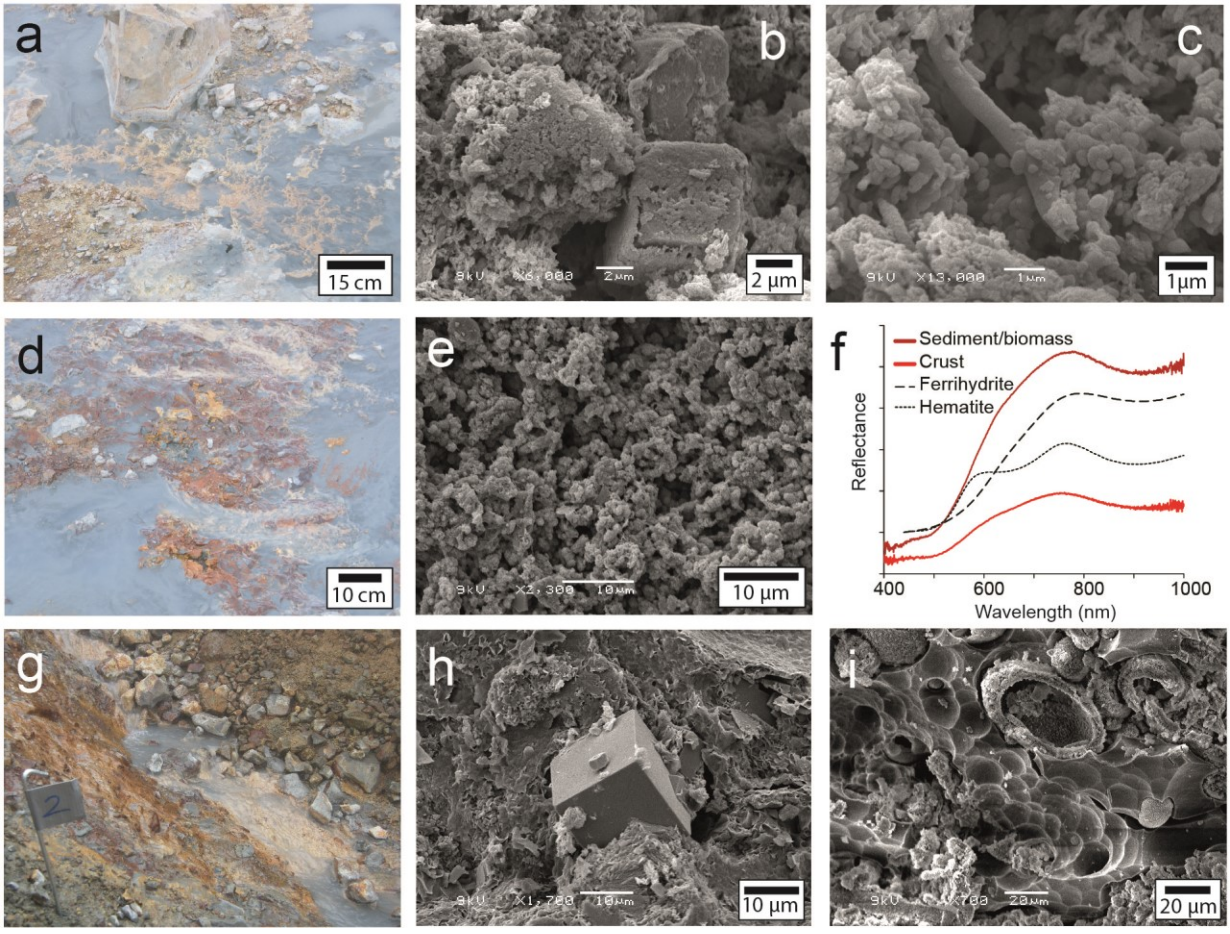

Figure 5. Dissolved SO_4^{2-} vs. sedimentary sulfide (as pyrite) within the hydrothermal pool (OF0), pool overflow stream (sites OF1 – 3) and red mineral terrace structures midway along the overflow (Red Crust).

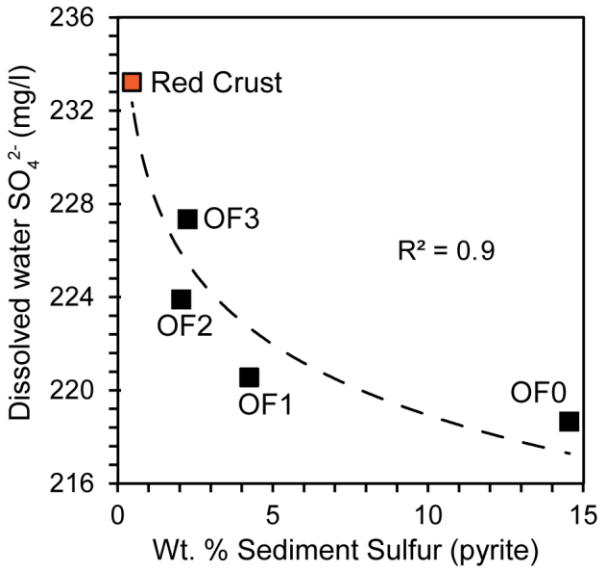

Figure 6. (a) Phylogenetic affiliation of 16S rRNA 454 pyrosequence data for Bacteria (Phylum level), **(b)** Phylogenetic affiliation of 16S rRNA Clone Library data for Bacteria, **(c)** Phylogenetic affiliation of 16S rRNA 454 pyrosequence data for Archaea (Order level).

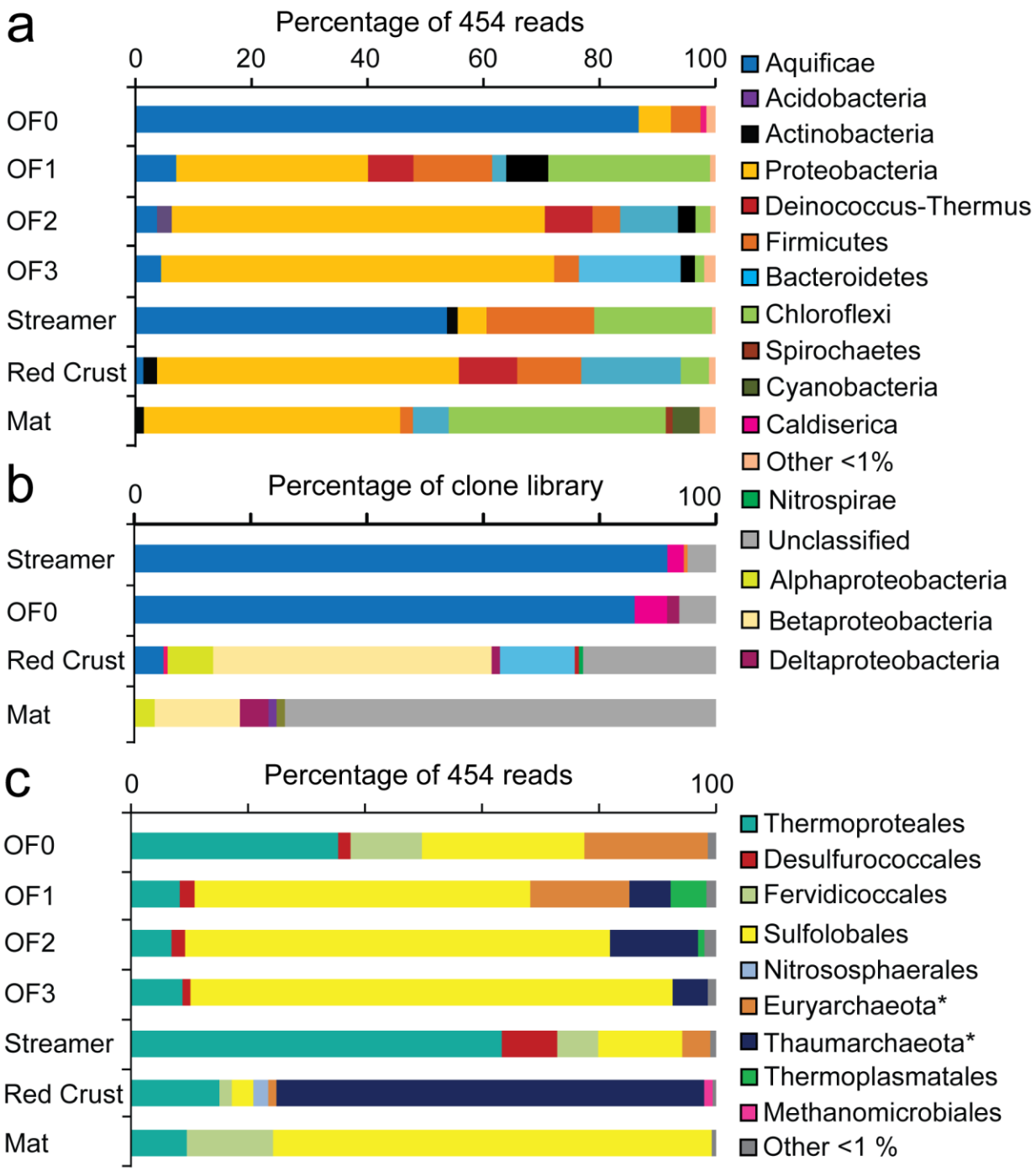

Figure 7. Phylogenetic tree of 16S rRNA clone library sequences from the OF0, Mat (Biomat), Red Crust, and Streamer sites.

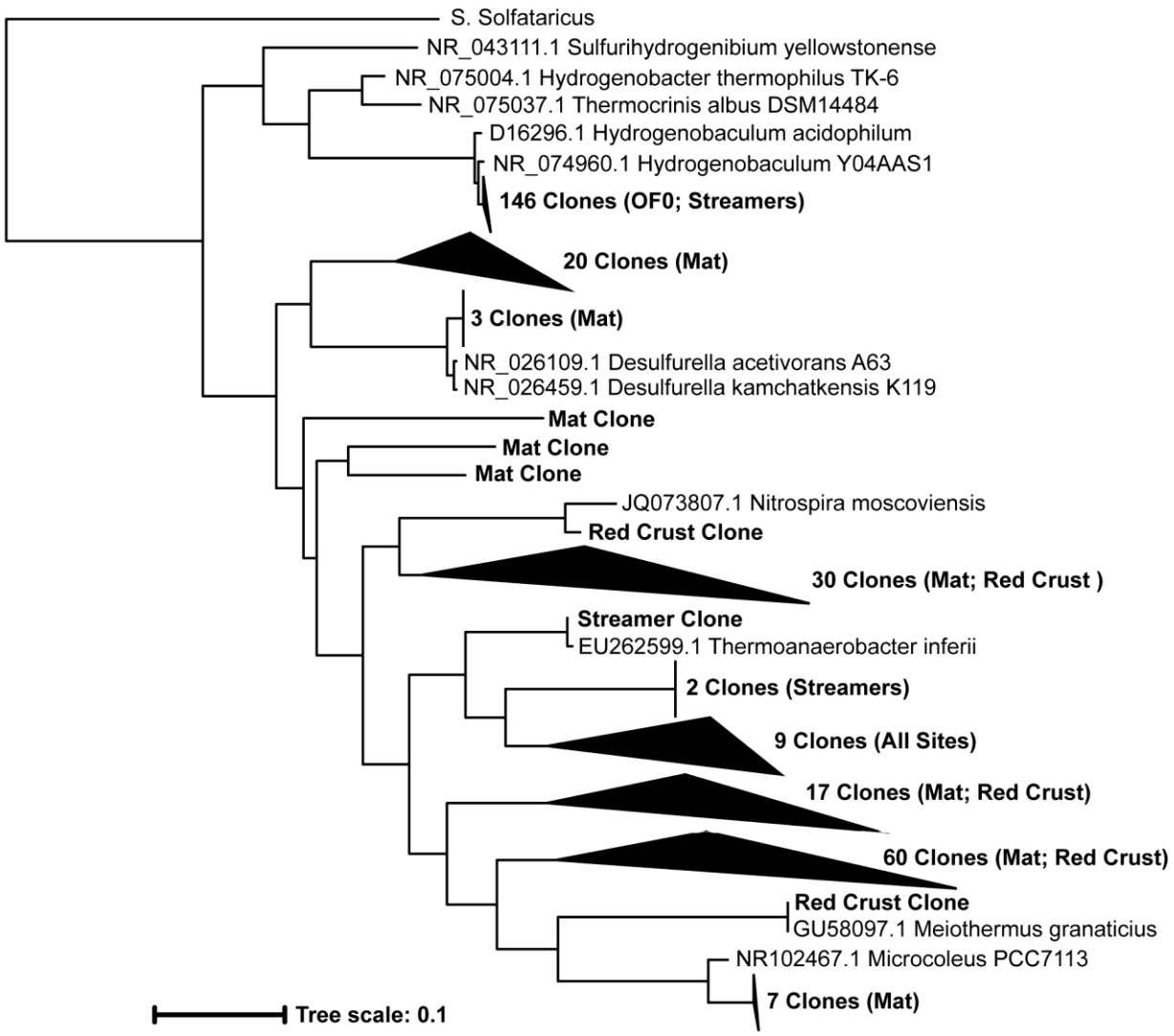

Figure 8. $\delta^{13}C$, $\delta^{34}S$, $\delta^{15}N$, and $\delta^{18}O$ stable isotope compositions for sedimentary Total Organic Carbon (TOC) and total fixed nitrogen, sedimentary pyrite, dissolved water sulfate, and Total Sulfur (TS) from microbial biomass and streamers, as a function of distance along the hot spring stream (see Figure 2). Error bars represent the standard deviation for each measurement (n=3), with some smaller than the point symbol.

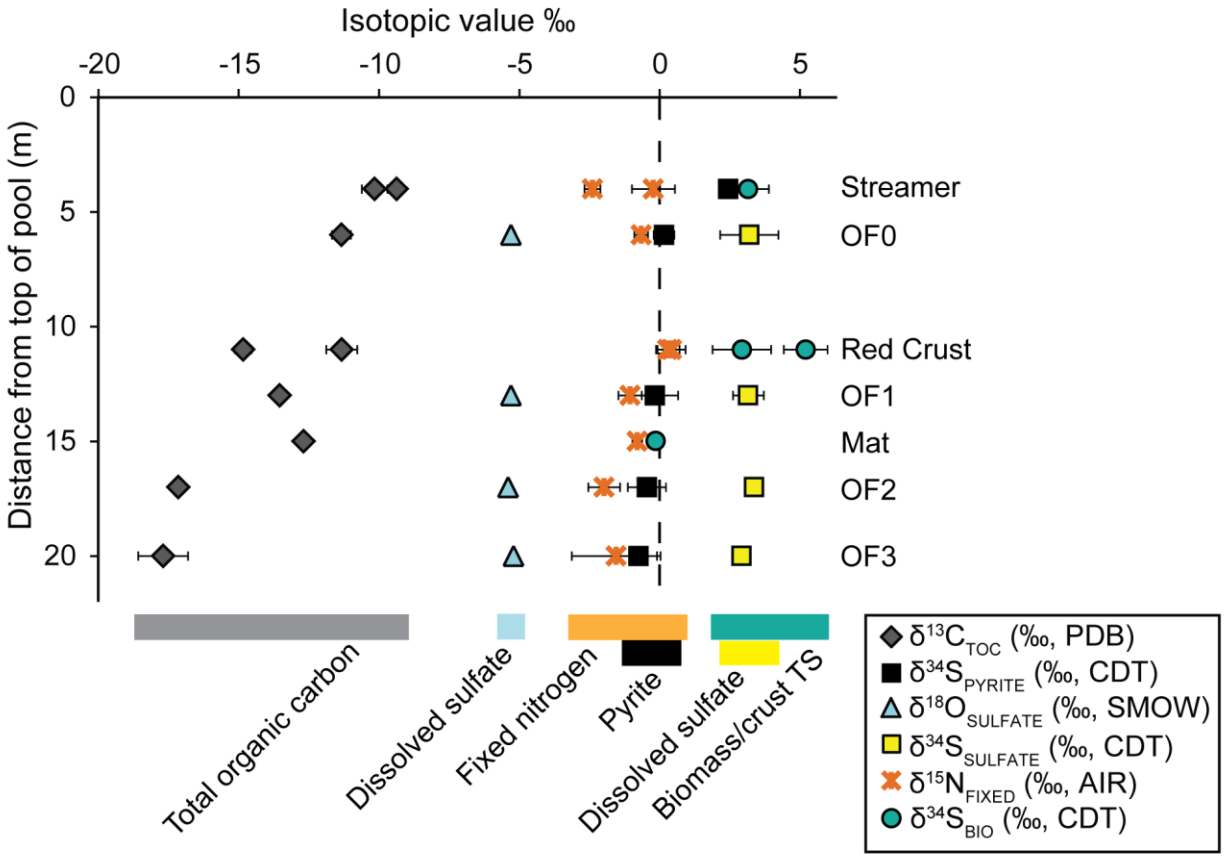

Table 1. Primers and PCR conditions used for screening of phylogenetic and functional genes (adapted from Weisburg *et al.,* (1991); DeLong (1992); Friedrich (2002); Scholten *et al.,* (2005); Hall *et al.,* (2008); Cockell *et al.,* (2011) and references therein) of which successful amplicons were produced for *NifH*, *APSr*, *mcrA,* and *Arch-amoA* genes.

Gene	**Primer sequence (5' – 3')**	**PCR Conditions**
16s rDNA	27F: AGTTTGATCCTGGCTCAG UN1492R: GGTACCTTGTTACGACTT Arch-21F: TTC CGG TTG ATC CYG CCG GA UNI1492R: GGTACCTTGTTACGACTT	95 °C for 4 min; 30 cycles of 94 °C for 30 s, 55 °C for 30 s, 72 °C for 1 min; 72 °C for 10 min
NifH	nifHF: GGHAARGGHGGHATHGGNAARTC nifHR: GGCATNGCRAANCCVCCRCANAC	94 °C for 2 min; 30 cycles of 94 °C for 30 s, 55 °C for 30 s, 72 °C for 30 s; 72 °C for 5 min
APSr	APSF: TGGCAGATMATGATYMACGG ARSR: GGGCCGTAACCGTCCTTGAA	94 °C for 2 min; 30 cycles of 94 °C for 2 min, 60 °C for 1 min, 72 °C for 3 min; 72 °C for 10 min
amoA	amoA 1F: GGGGTTTCTACTGGTGGT amoA 2R: CCCCTCKGSAAAGCCTTCTTC	94 °C for 2 min; 30 cycles of 94 °C for 30 s, 56 °C for 45 s, 72 °C for 45 s; 72 °C for 10 min
Arch-amoA	Arch-amoAF: STAATGGTCTGGCTTAGACG Arch-amoAR: GCGGCCATCCATCTGTATGT	94 °C for 2 min; 30 cycles of 94 °C for 30 s, 55 °C for 30 s, 72 °C for 30 s; 72 °C for 5 min
mcrA	MCR F: TAYGAYCARATHTGGYT MCR R: ACRTTCATNGCRTARTT	95 °C for 2 min; 30 cycles of 94 °C for 45 s, 50 °C for 30 s, 72 °C for 90 s; 72 °C for 5 min
dsrAB	dsrAB F: ACSCACTGGAAGCACG dsrAB R: GTGTAGCAGTTACCGCA DSR1-F+: ACSCACTGGAAGCACGGCGG DSR-R: GTGGMRCCGTGCAKRTTGG	94 °C for 1 min; 30 cycles of 94 °C for 30 s, 53 °C for 20 s, 72 °C for 1 min; 72 °C for 7 min

Table 2. Geochemical parameters of sampled sites along the hot spring stream. BD = below detection. DO = Dissolved Oxygen. "-" = not measured or not applicable. All values reported as mg/l unless otherwise stated. Standard deviations range between < 0.01 - 0.3 % (Al, Ca, Total Fe, K, Mg, Total P), 0.3 – 0.9 % (Na), and 0.09 – 3.2 % (Total Si). Measurement accuracy is ±0.1 for pH, ±0.1 °C for temperature and ±0.1 % for DO.

	OF0	**OF1**	**OF2**	**OF3**	**Streamers**	**Red Crust**	**Mat**
Environment	Pool	13 m Overflow	17 m Overflow	20 m Overflow	Streamers and crust	Red terraces and biomass	Microbial mat
Distance from top of pool/spring (meters)	6	13	17	20	4	11	15
pH	4.8	3.6	3.8	4.2	-	-	-
Temperature (°C)	53.2	40.2	37.1	34.7	68.0	-	-
DO	0-2	4.0	5.1	5.9	-	-	-
Total Fe	1.26	1.27	1.40	1.6	-	0.56	-
Total P	0.54	0.53	0.52	0.6	-	0.31	-
Total Si	91.66	90.78	108.54	119.9	-	93.06	-
Na^+	80.51	76.58	89.28	100.3	-	83.98	-
Ca^{2+}	26.79	26.99	33.36	37.2	-	29.19	-
Mg^{2+}	3.94	3.99	4.80	5.5	-	4.48	-
Total Mn	0.53	0.53	0.63	0.7	-	0.59	-
K^+	17.31	15.93	18.34	19.7	-	15.81	-
SO_4^{2-}	218.64	220.55	223.89	227.3	-	233.21	-
Cl^-	6.54	8.61	7.29	8.7	-	BD	-
F^-	1.76	1.73	1.57	3.3	-	1.70	-

Table 3. Sedimentary, biomass, and mineral crust Total Organic Carbon (TOC), Total Nitrogen (TN) and Total Sulfur concentrations and associated stable isotope values of sampled sites along the hot spring stream. N/A = not applicable. "-" = not measured. Analytical certainty ranges from ± 0.1 to 0.3 ‰.

	OF0	**OF1**	**OF2**	**OF3**	**Streamer**	**Red Crust**	**Mat**
TOC (wt.%)	0.25	0.23	0.08	0.07	1.81 (biomass) 0.34 (crust)	0.23 (sediment) 0.23 (crust)	2.40
Total N (wt.%)	0.04	0.04	0.01	0.01	0.34 (biomass) 0.063 (crust)	0.03 (sediment) 0.022 (crust)	0.29
$C/N_{(at)}$	6.73	7.02	8.64	10.11	6.30 (biomass) 6.49 (crust)	8.93 (sediment) 11.75 (crust)	9.41
Total S (wt.%)	14.56	4.25	2.06	2.27	1.96 (biomass) 23.57 (crust)	0.47 (sediment) 0.22 (crust)	6.07
TOC $\delta^{13}C$ (V-PDB) ‰	-11.34	-13.54	-17.15	-17.69	-9.37 (biomass) -10.16 (crust)	-11.33 (sediment) -14.84 (crust)	-12.69
Sedimentary TN $\delta^{15}N$ (AIR) ‰	-0.66	-1.05	-1.08	-1.55	-2.39 (biomass) -0.22 (crust)	0.42 (sediment) 0.29 (crust)	-0.8
Sediment/Biomass $\delta^{34}S$ (V-CDT) ‰	0.2	-0.2	-0.5	-0.8	3.2 (biomass) 2.4 (crust)	2.9 (biomass) 5.2 (crust)	-0.1
Dissolved sulfate $\delta^{34}S$ (V-CDT) ‰	3.2	3.2	3.4	2.9	-	-	N/A
Dissolved sulfate $\delta^{18}O$ (V-SMOW) ‰	-5.3	-5.3	-5.4	-5.2	-	-6.0	N/A

Supplementary File 1. Closest cultured match to 16S rDNA OTUs from sites OF0 (hydrothermal pool), Mat (microbial mat), Red Crust (red terrace sediment and biomass) and Streamer (microbial streamers). Major groups highlighted in bold

Closest match	**Identify %**	**No. of clones**	**Ecological characteristics (where defined)**
EF0			
Aquificae; Hydrogenobaculum	100	63	Thermophilic (45 – 80 °C), using H_2, H_2S or thiosulfate as energy sources and CO_2 for the carbon source (Romano et al., 2013 and references therein).
	98	59	
	97	1	
Deltaproteobacteria; Desulfurella	99	2	Thermophilic (45 – 80 °C), lithotrophic growth via sulfur or thiosulfate respiration or pyruvate fermentation, utilising H_2, organic acids and saturated fatty acids (Miroshnichenko et al., 1998).
	98	1	
Caldiserica; Caldisericum	100	3	Thermophilic (55 – 77 °C), anaerobic respiration using sulfur compounds (thiosulfate, sulfite and elemental sulfur), chemoheterotrophic (Mori et al., 2009).
	99	3	
	98	2	
Unclassified	82 - 94	9	N/A
Total Clones		*143*	
Mat			
Deltaproteobacteria; Desulfurella	100	4	See above
	98	3	
Betaproteobacteria; Thiomonas	100	3	Chemolithoautotrophs utilising reduced inorganic sulfur compounds, autotrophic and organotrophic growth, As(III) oxidation (Arsène-Ploetze et al., 2010 and references therein)
	99	3	
	98	2	
	96	1	
Betaproteobacteria; Thiobacillus	99	2	Obligate chemolithoautotroph; oxidation of inorganic sulfur compounds (Moreira and Amils, 1997)
	95	2	
Betaproteobacteria; Thiobacteraceae (fam.)	97	5	Not available
Alphaproteobacteria; Methylocystaceae (fam)	96	1	Type II Methanotrophs (Bowman, 2006)
Alphaproteobacteria; Acetobacteraceae (fam.)	96	4	Obligate aerobic respiration with O_2 as the terminal electron acceptor (Kersters et al., 2006)
Acidobacteria; Solibacterales (ord.)	95	2	
Cyanobacteria; Phormidium	92	2	Oxygenic photosynthesis, moderately thermophilic (28 – 45 °C) (Abed et al., 2002)

Betaproteobacteria; Methylophilales (ord.)	92	3	Aerobic heterotrophics, methylotrophy (Nakatsu et al., 2006)
Unclassified	78 - 91	106	
Total clones		*143*	
Red Crust			
Betaproteobacteria; Comamonadaceae (fam.)	100	2	Aerobic chemoorganotrophs or chemolithotrophs (H_2 or CO oxidation)
	99	1	that occupy a wide variety of environments (Willems et al., 1991)
	97	1	
Bacteriodetes; Sediminibacterium	100	5	Strictly aerobic or facultatively anaerobic heterotrophs (Kim et al.,
	98	13	2013)
Betaproteobacteria; Thiomonas	100	16	See above
	99	29	
	97	1	
	95	1	
Deltaproteobacteria; Desulfurella	100	1	See above
Deinococcus; Meiothermus	100	1	Thermophilic, aerobic respiration (Nobre et al., 1996)
Aquificae; Hydrogenobaculum	100	2	See above
	99	4	
	98	1	
Betaproteobacteria; Thiobacillus	99	1	See above
Caldiserica; Caldisericum	99	1	See above
Deltaproteobacteria; Syntrophobacteraceae (fam.)	99	1	Strictly anaerobic sulfate reducing bacteria, can have a syntrophic association with H_2-utilising bacteria (Kuever 2014)
Betaproteobacteria; Gallionella	99	2	Chemolithotrophic iron oxidising bacteria. Mixatrophic growth
	98	3	through CO_2 fixation and incorporation of simple sugars, with nitrogen
	96	2	sourced from nitrate and ammonium (Hallbeck and Pedersen, 1991)
Alphaproteobacteria; Rhodobacteraceae (fam.)	98	4	Aerobic sulfur-cycling photo- and chemo-heterotrophs, and anaerobic purple non-sulfur bacteria (Pujalte et al., 2014)
Nitrospirae; Nitrospira	98	1	Aerobic chemolithotrophic nitrite-oxidisers (Watson et al., 1986)
Betaproteobacteria; Thiobacteraceae	97	7	Not available
Alphaproteobacteria; Acetobacteraceae	96	5	See above
	95	2	
Betaproteobacteria; Methylophilales (ord.)	94	1	See above
Unclassified	79 - 95	32	N/A

Total clones		*140*	
Streamer			
Aquificae; Hydrogenobaculum	100	78	See above
	99	49	
	98	5	
Caldiserica; Caldisericum	99	4	See above
Firmicutes; Thermoanaerobacter	98	1	Thermophilic, anaerobic chemoorganotrophic thiosulfate reduction (Wagner et al., 2008)
Unclassified	79-97	7	N/A
Total clones		144	